

Analysis of Fatigue Behaviour of Superelastic Nitinol Wires

T.G.Gangadhar ¹, K.Manickavelan ², Balkeshwar Singh ³

^{1,2,3} Mechanical & Industrial Engineering Section,
Salalah College of Technology, Sultanate of Oman

Authors Email: tggangsadi@gmail.com ¹, k_manickavelan@rediffmail.com ², balkeshwar71@yahoo.co.in ³

Abstract

Shape-memory alloys exhibit reversible elastic response to an applied stress, caused by phase transformation between austenitic and martensitic phases of a crystal. Super elastic alloys belong to the family of shape-memory alloys. When mechanically loaded, a super elastic alloy may deform reversibly up to 10% by the creation of a stress-induced phase. The new phase becomes unstable upon removal of the load, returning the material to its original shape. Among the shape-memory alloys, NiTi alloys find wide use in engineering and medical applications. Straight annealed, super elastic, 1mm diameter NiTi alloy wire was subjected to characterization tests. Differential Scanning Calorimeter (DSC) tests were conducted to determine the Austenite start (A_s), Austenite finish (A_f), Martensite start (M_s), and Martensite finish (M_f) temperatures. Additionally, tensile and fatigue tests were conducted on the wire at ambient temperature for comparing the results with DSC data. The material exhibits close exothermic and endothermic peaks in DSC plots resulting in a cross over point at about 18°C. Therefore, the microstructure and mechanical properties of the alloy at this point are of interest. Phase transformation enthalpies derived from DSC tests were compared with loading and unloading resilience derived from tensile tests. The ratio of enthalpies was closely matching with the ratio of resilience, indicating that the material can be characterized by thermal or mechanical loading. Another observation was a marked step drop in stress level in the upper and lower plateaus of stress-strain plots beginning from the third fatigue cycle. This phenomenon was repeated during subsequent cycles, however at progressively lower strains, ending at the first inflexion point at the 23rd cycle. This information, when seen with published DSC data for similar materials, suggests occurrence of R-phase in the wire. The findings therefore lead to the conclusion that presence of R-phase in super elastic NiTi alloy can be detected by mechanical loading tests.

Key words: superelastic, alloys, fatigue behavior, tensile test, fatigue test

I. INTRODUCTION

Shape memory alloys were discovered as early as 1932 and until 1971 it was believed to be common to all alloys that undergo thermoelastic martensitic transformations. However, it was realized that only specific alloys showed Shape memory Effect (SME) and Super elasticity (SE) behavior and considerable efforts are

made to discover more such materials with tailored properties. Of these alloys, however, only two alloy systems, CuZnAl and NiTi, and their combinations with minute quantities of other elements are presently of commercial importance. The properties of NiTi and CuZnAl alloys are fairly different, due to their different micro-structure. Because NiTi alloys have much higher strength, larger recoverable strain, better corrosion resistance and most importantly higher reliability than CuZnAl, they are the preferred for space and other application. SMAs have been used in a wide variety of space applications because of their unique thermo mechanical characteristics. The advantage of using SMA is that after severe deformation, SMA can still fully return to its original shape due to its excellent superelasticity. *Future launchers* will have larger envelope and mass capabilities, but large elements, such as solar arrays, antennas and large frames or masts etc., still cannot be taken into orbit in their operational configuration. The only solution is to make these structures foldable and to deploy them into their operational configuration in orbit. Furthermore, in the case of large structural elements the number of launches required to place them in orbit, and the number of in-orbit assembly operations, either by astronauts or by service vehicles, can be minimized if deployable structures are used. Instead of traditional actuator, cable or folded structure, SMA can be used in these deployment schemes with very smooth motion due to its inherent damping properties. SMA based deployable structure can be folded easily by large deformation of SMA. During deployment, SMA is heated to above its transformation temperature to recover its original shape. The advantages of SMA-deployed structures over existing solutions are mass and volume savings, avoidance of end-of-deployment shock loadings, retraction capability, noiseless operation, sensing capability. higher reliability, large recoverable strains, high electrical resistivity, & design flexibility. Xin Lan, Jinson Leng, Shanyi [1] designed deployable structure, it is necessary that a relative movement, i.e. a rotation or a linear motion, occurs between different parts of that structure. Such movement can be generated either by a specially designed actuator or simply by a part of the structure changing its shape.

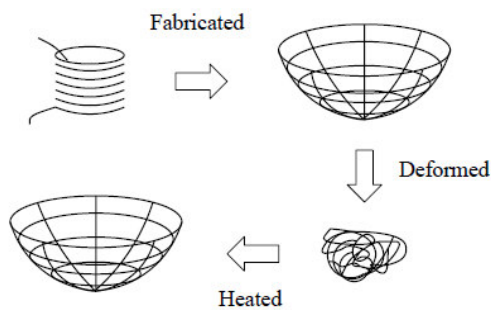


Figure 1(a): (from Gandhi and Thomson 1992 [1])

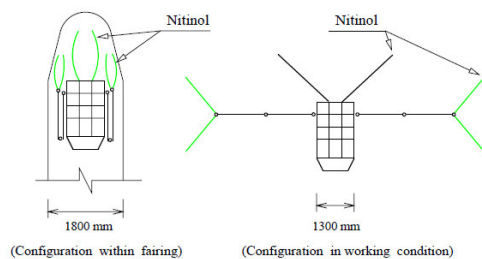


Figure 1(b): (From Yang et al. 1985 [2])

Structures made of SM alloys

Figure 1(a) & Figure 1(b) shows SMA satellite structures made of Nitinol wire. In recent years, SMAs were used for off loading system of the Hubble space telescope solar array drive in a no-shock separation

mechanism for spacecraft release in a multi-shot deployment mechanism for both release and spring recharge to open the cover glass of a solar cell of NASA's Mars Path Finder Rover, as shown in Fig. 2 [3].

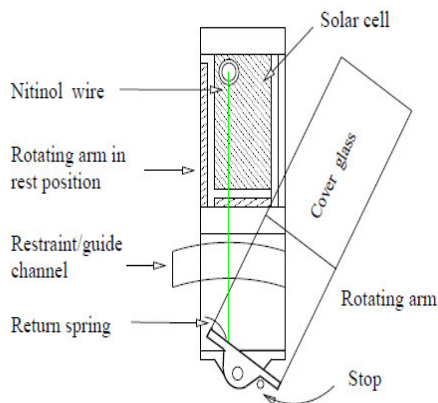


Figure 2: SMA-Actuated Rotating Arm (from Jenkins and Landis 1995[3])

Nitinol mast, which is similar to the masts made by the Astro Aerospace Corporation and by AEC-Able Engineering, but, instead of being driven by an electrical motor, have their vertical members released by actuation of Nitinol, similar to the Storable Tubular Extendible Member (STEM). The similar actuation was tested on board of the spacecraft PROGRESS-40 to deploy space truss which contained five transformable units. Each unit consisted of four hinged panels, as shown in the Figure 3, The wire is a 2 mm diameter Nitinol heated by passing an electric current through it[3]. The use of SMA torsion springs figure 4, also heated by passing an electrical current through them has been suggested as a way of deploying solar panels.

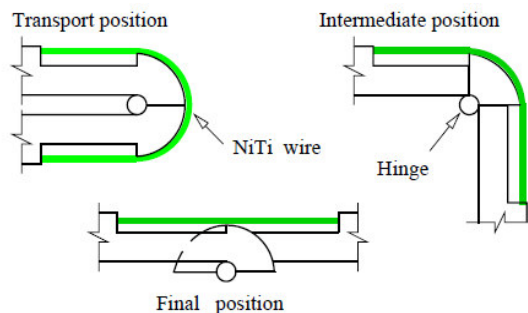


Figure 3: SMA hinges (From Likhachev, et al 1994[4])

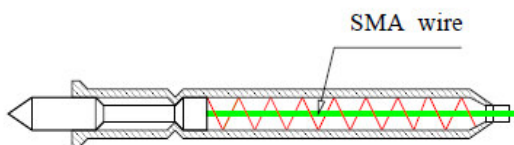


Figure 4: linear motion SMA actuator (From Moorleghem 1993[5])

Figure 5(a), 5(b) & 5(c) shows the design of a new deployable antenna actuated by 6 shape memory alloy (SMA) hinges.

The antenna designed by Xin Lan, Jinson Leng, Shanyi[6] consists of 6 radial, tensioned, parabolic, deployable ribs connecting to a central hub. The hinge, located at each rib, is made of Nitinol SMA Material due to the ability to generate large strains under electrical resistive actuation. The elongated SMA wire is

heated by an electrical current, caused to contract in response to a converse thermally-induced phase transformation. The resulting tension creates a moment, imparting rotary motion between two adjacent beams. The deployable truss consists of six radial, tensioned, deployable ribs connecting to two central hubs on the center axis. Each rib with the shape of triangle and parallelogram contains four beams. Beam 1 is connected to the upper hub, and beam 2 is connected to the lower hub. The upper hub is fixed on the center axis, and the lower hub can move along the center axis. When the lower hub moves towards the upper hub, one side of triangle contracts, the parallelogram deploys at the same time, and the truss structure deploys from stowage to deployment.. Results indicated that the hinge with low speed rotation and easy fabrication achieves reliable actuation for the deployment of the antenna, and the antenna demonstrates a high deployment-to-stowage volume ratio.



Figure 5(a): Deployable Antenna Actuated by Shape Memory Alloy Hinge

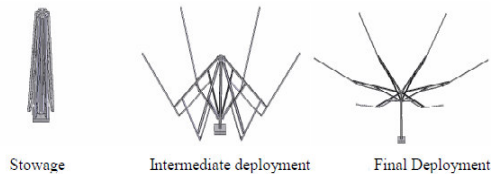


Figure 5(b): Process of deployment for the deployment truss

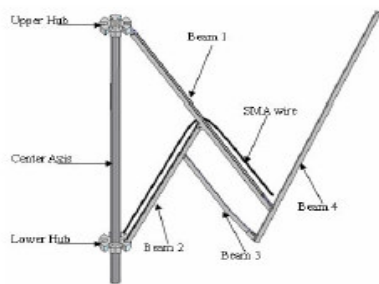


Figure 5(c): Deployable rib element for truss

Quantitative experiments were conducted on a new type of actuator that uses shape memory alloy (SMA), which was developed for the solar paddle of small satellites. The actuator can orient the solar paddle alone toward the sun, and is equipped with a counterweight to compensate for the rotating motion of the small satellite in microgravity. The actuator measures 100 mm in diameter and 127 mm in height, and weighs approximately 660 g including the counterweight (340 g). To rotate the solar paddle, six SMA springs, each of which has a cylindrical mirror in the rear in order to concentrate the sun's energy onto the spring. More 10

power can be generated if a deployable solar paddle and a solar tracking mechanism are used. However, the number of small satellites using a deployable solar paddle is small. The actuator can rotate 360 degrees continuously and orient the solar paddle alone toward the sun. It is equipped with a counterweight in order to compensate for the rotating motion of the small satellite in microgravity. To rotate the paddle, we used six SMA springs, each of which is made of 0.8-mm-diameter wire and has 10 turns; the coil diameter is 5.8 mm and the mass is 0.8g. Each spring has a cylindrical mirror in the rear in order to concentrate the sun's energy onto the spring. The type of SMA is TiNi (Ni 55.2 wt %) alloy and the transformation temperature is approximately 57°C.

II. SPECIMEN

Ni-Ti alloy wires were procured from Alfa-Aesar, USA. The data sheet provided by the supplier had the following information, Ni-Ti wires, 1 mm diameter, superelastic, Alloy N, straight annealed, oxide surface with active Af of 9 deg.C and Ingot Ap of -19 deg.C, upper plateau of 80 ksi and lower plateau of 30 ksi, elongation of 21%, tensile 205 ksi and breaking load of 244 ksi. Differential Scanning Calorimeter (DSC) tests were conducted on this wire to determine As, Af, Ms and Mf temperatures, the heating and cooling rates were 10°C/min. Tensile and cyclic fatigue tests were carried out using a 10kN, computer controlled servo-hydraulic universal testing machine with bollard grippers. Tests were done with two different span or gauge lengths, 150 mm and 300 mm, the strain rate was kept constant at 3 mm/min and the tests were conducted at ambient temperature and pressure conditions.

III. EXPERIMENTAL SETUP

The experimental set up that will be conducted by the UTM is shown in the figure. The Nitinol wire was pulled at cross head speed of 3mm/min at room temperature (26°C). Displacement of the wire was measured by the movement of the cross head speed. The value of force reading was measured by the 5KN transducers. The Nitinol wire was held by the bollard grippers of the universal testing machine. The value of the force reading was set to zero using computer controlled machine. When the force was set to zero the displacement position of the cross head and room temperatures was noted. Using the cross head movement the change in length and stress were recorded using the computer controlled UTM on continuous basis. For fatigue testing we have repeated 10 numbers of cycle (N=10) and stress induced transformation was noted down during loading. Unloading was carried out manually using computer controlled UTM where cross head moves towards downward at the rate of 3mm/min, the experiment was repeated for 10 cycles.

IV. RESULTS & DISCUSSIONS

Ni-Ti alloys undergo phase transformation with change in temperature or change in stress. Typically Ni: Ti is in the ratio of 55:45 wt%, and these materials display solid-solid transition, which is a transformation from one crystal structure to another. There are different types of solid-solid transitions reported in literature. Most often NiTi alloys undergo transformation from BCC (austenite) to monoclinic (martensite) structure, however this is not true in all the NiTi alloys, since they are extremely sensitive to alloying elements and microstructure (combination of processing and heat-treatment). Differential scanning calorimeter is one instrument that can detect solid-solid phase transformation as a function of temperature only. Figure 6 shows a typical DSC plots NiTi alloy, the top portion of the curve arises during cooling cycle and the bottom portion of the curve arises during heating. Figure 7 shows the DSC plot of as received superelastic grade nitinol wires. Unlike most DSC plots reported in literature, this plot has some temperature values. Upon cooling from room temperature the Ms temperature was recorded at 24.23°C, Mp=10.87°C

and $M_f = -0.93^\circ\text{C}$. And on heating the austenite start temperature A_s was observed at -10.67°C , $A_p=6.30^\circ\text{C}$ and $A_f=27.15^\circ\text{C}$.

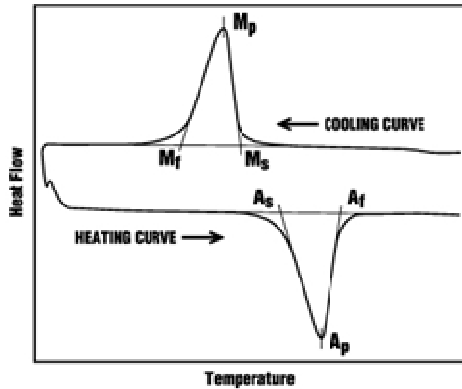


Figure 6: Typical Differential Scanning calorimeter (DSC) Plots of Ni-Ti Alloys

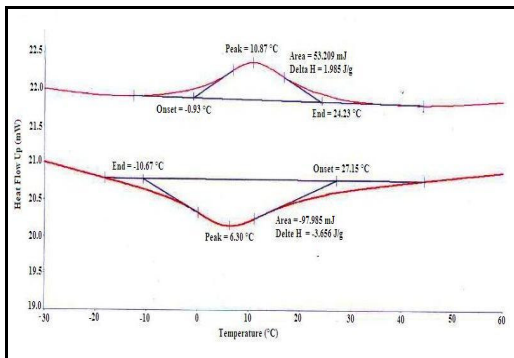


Figure7: DSC Plot of as received Superelastic Ni-Ti wires, the top line corresponds to cooling cycle (martensite phase) and the bottom line corresponds to heating cycle (austenite phase)

These experiments were repeated more than once and the results were corroborated with those reported by Memry Corporation. The enthalpy for austenite to martensite transformation is $+1.98 \text{ J/g}$ and for reverse transformation is -3.65 J/g . The DSC plots are also represented in the form given in Figure 8, to determine the hysteresis loop. The difference between the exothermic and endothermic peaks is considered as the width of the hysteresis loop. In case of the Ni-Ti alloy, presently under study, a cross-over point is observed at 18 deg.C . The material characteristics at this point, and its effect on the properties, microstructure needs further investigation.

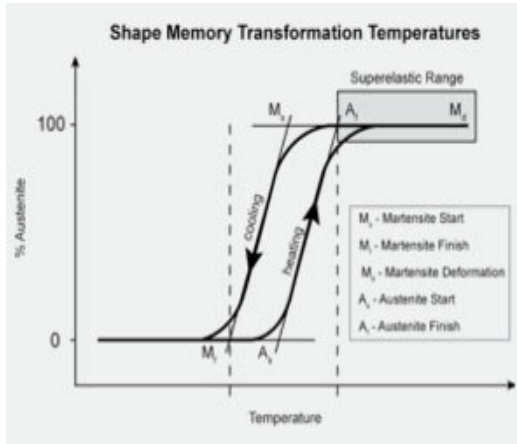
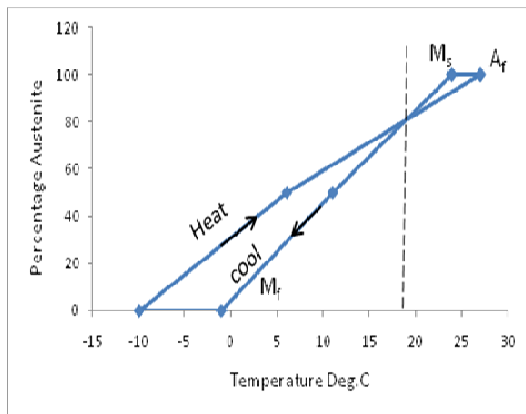


Figure 8(a): Typical Hysteresis Loop of Ni-Ti Alloy



(b)

Figure 8(b): Hysteresis Loop of the Ni-Ti Alloy used in the present study.

The solid-solid transition occurs in steps, characterized by an intermediate phase formation. In literatures [7,8,9], BCC to monoclinic transformation has been reported with the formation of intermediate phases which in some cases is orthorhombic and in some cases rhombohedral or even tetragonal. A full atomic level Ni-Ti solid-solid transition is yet to be understood. Calculations based on first principles, specifically based on density functional theory (DFT) [10,11] are proving to be reliable for prediction of crystal structures. Figure 4 gives the crystal structure of solid-solid phase transition from BCC to Monoclinic via intermediate phases. These transformations are not necessarily temperature dependent, they can be brought about by applying stress or a by applying a combination of stress and temperature.

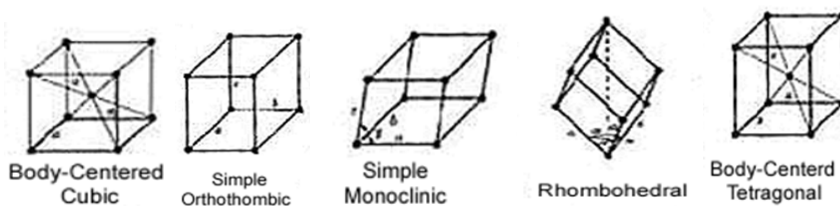


Figure 9 (a): Different Possible Solid-Solid Phase Transitions in Ni-Ti Alloys as a function of Temperature or Stress

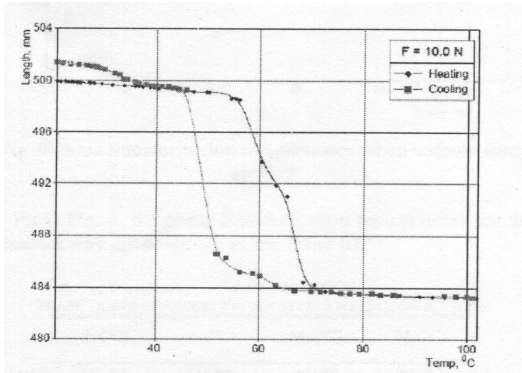
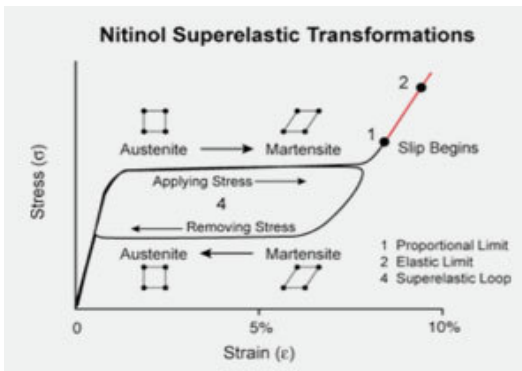
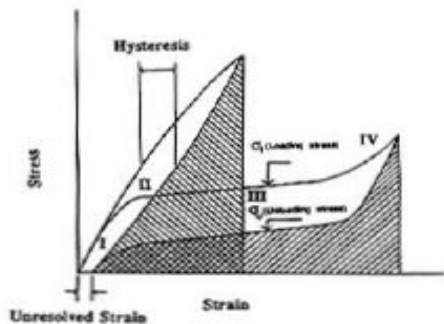


Figure 9(b): Transition by a Combination of Stress & Temperature.

Figure 10 shows the typical stress-strain and cyclic load test results of Ni-Ti alloys[12,]. The unique characteristic of this class of materials is the elastic limit. It has a non-linear elastic region and a plateau region (labeled I and II- Figure 10(b)), which corresponds to austenite phase and a gradual stress induced transformation to martensite phase (region marked III- Figure 10(b)). This elastic region is followed by martensite elastic region (marked IV in Figure 10(b)), beyond this point slip planes begin to appear causing plastic deformation (marked 1 in Figure 10(a)), further loading of the material will lead to severe plastic deformation and finally failure. The failure strain for most materials in this class is beyond 20% strain. Tensile tests were conducted on the 1 mm diameter as received Ni-Ti wires using a computer controlled servo-controlled 10kN universal testing machine with bollard type grippers and a strain rate of 2% of the gauge length as specified in ASTM F2516-07e2. Table 1 gives the failure strain, resilience values.



(a)



(b)

Figure 10: Typical Tensile & Cyclic Loading Test Results of Ni-Ti Alloy

Gauge Length	Elastic Region				Resilience
	Stress	Strain%	Stress	Strain	
150mm	460MPa	3%	540MPa	10.5%	47 MPa

Table 1: Properties of Ni-Ti Alloy Wires Computed from the Strain-Strain Plot from Figure 11

By simultaneously considering Figure 11 and 10 (b), the following inferences can be drawn (1) at 3% strain and a stress value of 460 MPa the Ni-Ti wire shows the first inflexion point, and the relation between strain and stress from 0 to 3% is non-linear. Thus, upon unloading, a hysteresis loop will be formed. The area of envelop will indicate the energy stored, absorbed or dissipated through a process of crystal structure modification or will result in increase in temperature. (2) The second inflexion point is observed at 11% strain and at a stress value of 540 MPa. The region between the first and second inflexion point is labeled as 'upper plateau'. During loading, the area under the stress strain curve is the strain energy per unit volume absorbed by the material and in this case it is 43 MPa. Conversely the area under the unloading curve is energy released by the material and it is 22 MPa. The difference in energy, which is 19MPa is partly absorbed and partly dissipated as heat.

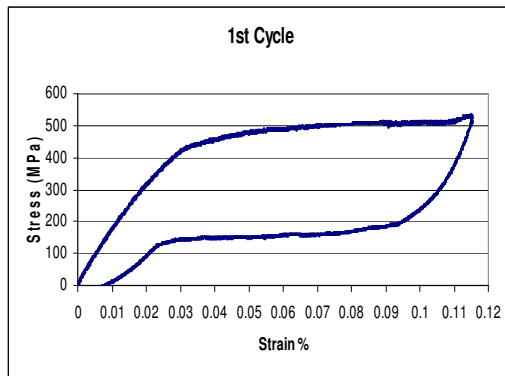


Figure11: Tensile Test Plots of Ni-Ti wires 150 mm gauge length with a Strain Rate of 3mm/min

Figure 11 and Figure 8 are equivalent, in the former the solid-solid phase transition occurs due to stress and in the later it is due to temperature. The energy equivalent values compare well between the tensile and DSC tests as shown in Table 2. The ratio of the energy absorbed during heating and cooling in DSC test is 1.85 and is comparable to the ratio of energy during loading and unloading. The slopes of the three inclined portions of the curve in Figure 6 are similar with a modulus of 12000 to 16000 MPa

DSC Test	Enthalpy (ΔH) (J/g)	Tensile Test Elastic Limit	Resilience MPa
Martensite (Ms to Mf)	1.98	Loading	43 MPa
Austenite (As to Af)	3.65	Unloading	22 MPa
Ratio	1.85		1.95

Table 2: Comparison between DSC Data and Tensile Test Data

Figure 12 shows the plots of super elastic Ni-Ti alloy wires subjected to fatigue cycles. The plot shows the 1st, 5th and 10th cycle. Table 3 gives the corresponding stress-strain values for each of the three cycles shown in the Figure 12. In the 5th cycle a step is observed along the upper plateau at approximately 8% strain and in the 10th cycle at approximately 6.5% strain. This observation is combined with the DSC plots shown in Figure 8, taken from [13]. In the first cooling cycle, a single exothermic peak is observed for Ms to Mf, however in the 10th cycle the peak intensity reduces and also a shoulder appears to the right side of the peak, broadening the transition temperature zone. In the 23rd cycle the peak intensity is further reduced and the shoulder width is increased even further. The area within the load-unloading curve reduces from 27MPa to 21 MPa

Gauge length	Forward Transformation				Reverse Transformation			
	Stress (MPa)	Strain %	Stress (MPa)	Strain %	Stress (MPa)	Strain %	Stress (MPa)	Strain %
150 mm	440	3.2	480	11.5	195.32	9.38	138	3
First cycle	365	3	440	11	157.5	8.75	110	2.78
Fifth cycle	350	2.9	420	10.6	123	8.2	103	2.61
Resilience	First cycle		Fifth cycle		Tenth cycle			
	27.615		27.615		27.615			

Table 3: Stress-Strain Values as a Function of Fatigue Cycle, corresponding to Figure 7Fatigue

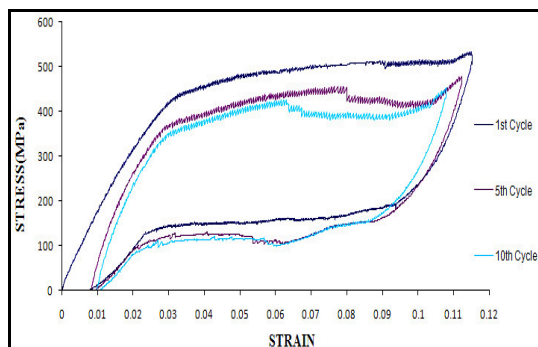


Figure 12: Plots Stress-Strain of Ni-Ti alloy Wire Subjected to Fatigue Cycles 1, 5 and 10 cycles.

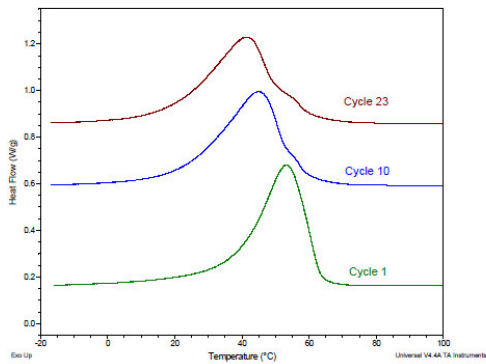


Figure 13: Growth of R Phase in Ni-Ti Alloys Due to Thermal Cycling using DSC Instrument.

The inferences that can be drawn from the stress fatigue and thermal fatigue cycle results are (a) the BCC to monoclinic transition shown in Figure 4(a), begin to become more complex, the appearance of the shoulder in Figure 8 and a step in Figure 7 along the upper plateau region, indicate the occurrence of R phase (b) the upper and lower plateau gradually shifts downwards by about 100 MPa by about 10th cycle, indicating a combination of microstructure changes along the grain boundaries, twinning and de-twinning, R phase, resulting in considerable reduction in internal energy.

V. CONCLUSION

Ni-Ti alloys are a unique class of materials, whose properties and behavior are far from being understood. Superelastic Ni-Ti alloys have distinct properties when compared to shape memory Ni-Ti alloys. The solid-solid phase transition can be achieved by thermal or mechanical or by a combination of thermal and mechanical. Recoverable elastic strains of nearly 10% were observed in the present study, with a corresponding stress value of 450 MPa. Fatigue cycling induced significant micro structural changes along grain boundaries, twinning/de-twinning of martensitic structure and even occurrence of R phase.

Acknowledgement

The authors wish to acknowledge the services provided by Dr. Bhaumik S.K, National Aerospace Laboratories, Bangalore for DSC measurements and Mr. M Virupaksha, Bangalore Integrates System Solutions, Bangalore for assistance in conducting the fatigue testing experiments. We are also thankful to Mr. N. Sellappan, HOS of Mechanical Engineering, Dr. Said Mohammed Al-Mashikhi, Head, Department of Engineering, and Dr. Maryam AlAwadi, Dean, Salalah College of Technology for their valuable inspiration, encouragement and providing necessary facilities for the study.

References

- [1] Gandhi M.V and Thomson B.S.(1992), *Smart Materials and Structures*, Chapman & Hall.
- [2] Yang, H., Liu, Z.C and Tang, L.L(1985), "Antenna Made by Shape Memory Alloy for TW-1 Satellite".
- [3] Jenkins P.P and Landis G.A (1995) "A Rotating Arm Using Shape-Memory Alloy, 29th Aerospace Mechanisms Symposium, NASA conference Publication 3293, pp 167-171.

- [4] Likhachev, V.A., Razov, A.I., Cherniavsky, A.G., Kravchenko, y. and Trusov, S.N.(1994), "Truss Mounting in Shape memory alloys, Proceedings of the First International Conference on Shape Memory and Superelastic technologies, California.
- [5] Moorleghem, W.V.(1993), The Use of Shape Memory Alloys in Space Structures, Either as an Actuator or as a Passive Damping Elements, Space Structures 4, London pp 833-842.
- [6] Xin Lan, Jinson Leng, Shanyi " Design of a Deployable Antenna Actuated by Shape Memory Alloy Hinge"Material Science forum volume 546-549(2007).
- [7] Warren j. Moberly, T.W. Duero, J Profit and r. Sinclair "Two Step Martensitic Transformations in TiNi(10% CU) Shape Memory Alloys".
- [8] WJ. Moberly, PhD Thesis: "Mochanical Twinniog aod Twinless Manensi!e in Ternary TiNi Alloys", Stanford University, (1991).
- [9] O. Mercier, K.N. Melton, R. Gotthardt and A. Kulik, "Solid- Solid Phase Transformation" p1259-63 (1982).
- [10] Xiangyang Huang, Graeme J. Ackland & Karin M. Rabe "Crystal structures and shape-memory behaviour of NiTi" Nature Materials 2, 307 - 311 (2003).
- [11] Kudoh, Y., Tokonami, M., Miyazaki, S. & Otsuka, K. " Crystal Structure of the Martensite in Ti-49.2at %Ni alloy analysed by the single crystal X-Ray diffraction method. Acta Metall, Mater.33, 2049-2056.
- [12] Zadno, Duerig, "Linear and Non-Linear Superelasticity in NiTi" MRS Shape Memory Materials Vol. 9 pp. 201-209.
- [13] Carlton G. Sloough "A Study of the Nitinol Solid-Solid Transition By DSC" TA Instruements, 109 Lukens Drive, New castle, DE 19720, USA.